Characterizing GPS Signal Deformations using the WAAS Signal Quality Monitor

R. Eric Phelts and Todd Walter, *Stanford University*

Abstract

This paper develops a method to estimate and characterize GPS codes distortions using WAAS signal quality monitor data. It leverages previously proposed signal models to map monitor metrics into generalized model waveform parameters that best approximate the signal. The modeled waveforms are then used to analyze signal characteristics and generate range error estimates that can be used to assess the assumptions for GPS signals and WAAS monitor performance. This includes comparisons to specifications for nominal GPS signal deformation and also assumptions for acceptable WAAS user range errors in the presence of one anomaly event. It is shown that these assumptions continue to hold and that this method may provide a complement to high-gain dish antenna measurements for assessing the effects of signal deformations in GNSS receivers on an ongoing basis.

1. INTRODUCTION

Signal deformations are subtle distortions of GNSS signals relative to each other. The best assessments of signal deformations and their effects traditionally derive from measurements made with large, high-gain, directional dish antennas. (Thoelert, S. et al, 2015, 2020; Wong, G. et al 2010, 2014) These measurements, combined with high-resolution, signal analyzers, allow the full, raw RF signals to be digitized at a high sample rate. Correlation peaks can be formed from the processed raw data, and the signals can be analyzed in receiver models to determine their impact on signal deformation monitors and user receivers (e.g., range errors).

These high-quality measurements are somewhat limited, however. The highly-directional antennas can only capture signals from a single SV at a time. Also, the records are usually very short (e.g. only a few seconds) in duration. In addition, because the antennas are often specialized and accessible by relatively few people or organizations, the data is often costly and/or difficult to obtain. These limitations mean this data is best suited for capturing nominal performance sporadically and is unlikely to be available to capture transient or anomalous behavior, which may not persist long enough to acquire more detailed observations of the signal.

The Wide Area Augmentation System (WAAS), however, continuously monitors the GPS signals using wide-bandwidth, multi-correlator receivers distributed across North America. Accordingly, WAAS observes (L1 and L5) signals from roughly half the GPS satellites on orbit at any given time. It also records and stores the receiver outputs indefinitely. (Phelts, R. E. et al, 2022) As a result, the WAAS signal quality monitor is far more likely to capture anomalous signal behavior when it occurs.

This monitor is also limited in that it only observes the (front-end filtered) correlation peak of the signal. Also, the samples of the peak are relatively few. WAAS monitor receivers also do not have the high gain and directionality of large dish antennas, but instead rely on averaging across receivers to reduce noise. While quite effective, this does not mitigate the effects of ground multipath as well. Still dish measurements have been used to compliment this WAAS signal monitor data analyses. (Phelts, R. E. et al, 2015)

Estimates of WAAS monitor metrics can be computed from the dish data to characterize the signals at that instant in time. Combined with models of allowed WAAS user receivers, these results have been used to model expected user range errors due to nominal signal deformations, which are generally quite stable over time. (Pagot, J. B., et al 2015; Phelts, R. E. et al, 2015,

2022) In addition, models of both nominal and anomalous deformations have been proposed to estimate WAAS monitor metrics and user receiver errors. These signal models have also been directly compared to the measured dish waveforms. (Phelts, R. E. et al, 2015, 2017)

The method proposed in this paper introduces a modified signal model to better characterize both nominal and previously-observed anomalous waveforms. Then it presents a method to use the WAAS signal quality monitor detection metrics to estimate the model parameters that best characterize the waveform shape. Such a technique would be useful for 1) continually confirming nominal signal characteristics comply with assumptions over time, and 2) verifying that current signal deformation threat model and monitor continues to protect against real-world threats.

2. BACKGROUND:

1. Characterization Approaches

1. "Exact" Measurements (Dish Data)

High-gain dish measurements are best for capturing the fine details of the code. And, after conversion to I/Q samples and carrier removal, the codes can easily used to model receiver behavior. However, while exact, they are not readily generalizable and provide limited connection to the standard threat model—the ICAO 2nd-Order Step model. [Thoelert, S. et al, 2015; Phelts, R. E. et al, 2017]. In fact, digital distortion—advance or delay in the timing of the falling edges of the code chips—can be directly measured by these measurements (Wong, G. et al, 2010), but the analog deformation parameters of that model cannot.

Figure 1 plots of two sets of dish measurements on L1 C/A code. The first set was taken in 2010 and has been used extensively in previous characterization analyses by Wong, G. et al (2010) and Phelts, R. E. (2015, 2022). Additionally, 13 traces from 2020 are plotted. This more recent dataset is not as complete as the first but are the measurements used to tune the models and to demonstrate the characterization method described in this paper.

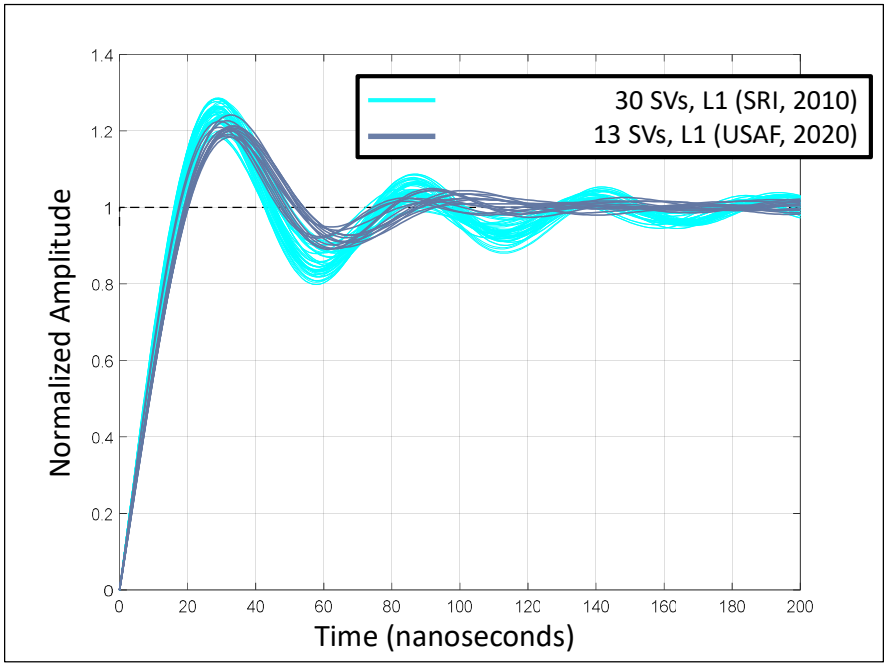

Figure 1. *High Gain Dish Measurements for L1 C/A code*

2. Step Response Performance Parameters

Specifications like rise time, settling time, peak time, and maximum percent overshoot are a standard way for specifying limits on 2nd-order system. They were proposed by Phelts, R. E. et al (2009) as a way to constrain and specify nominal deformation parameters in order them from anomalous signals. However, these are too general to sufficiently describe typical subtle nominal and near-nominal signal shapes. This is because the latter are not well-characterized by a second order step model.

3. ICAO 2nd-Order Step Threat Model

The ICAO 2nd-Order Step (2OS) model is the standard model for designing robust signal deformation monitors and for certifying that GNSS augmentation systems are safe against signal deformation threats. It was introduced long ago and has been discussed extensively in the literature for many years. (Phelts, R. E., 2001)

The 2OS model is a compact, three-parameter representation of the features common to the chip shape—damped frequency of oscillation (f_d), damping factor (σ), and digital distortion or led/lag of the falling edges (Δ). (See Equation (1).) However, this mostly focused on more extreme threats and correlation peak distortion. And it has served to design very robust monitor detection algorithms rather than to capture the subtleties of nominal distortion of the code shape.

The transfer function for the 2OS analog distortion is given by

$$H_d(s) = \frac{(\omega_0)^2}{s^2+2\zeta\omega_0 s+(\omega_0)^2} \tag{1}$$

where

$$f_d = \frac{1}{2\pi}\sqrt{1-\zeta^2} \tag{2}$$

and

$$\sigma = \zeta\omega_0 \tag{3}$$

The two-parameter analog portion of the model is limited both in its parameter limits and its model order. In particular, the upper bound on parameter σ is not large enough to reduce the amplitude to typical nominal ranges. In addition, oscillation frequency f_d is coupled with the amplitude overshoot of the step response. This limits its ability to match real-world observations of multiple performance parameters simultaneously.

Figure 2a illustrates the 2OS waveform for the first few chips of a typical C/A code sequence. Figure 2b plots one of the waveforms corresponding to the parameter limits of the model for f_d and σ. The latter is compared to nominal step responses as measured by the (2010) high-gain dish data from Figure 1. The maximum damping factor σ is too small at the upper limit of the 2OS model range ($\sigma_{max,2OS}$=8.8 MNepers/s) to reduce the overshoot to levels comparable to nominal responses.

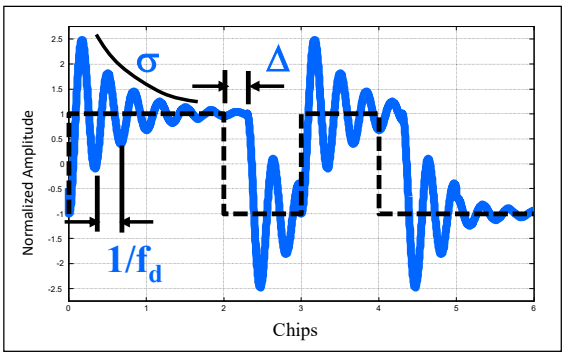

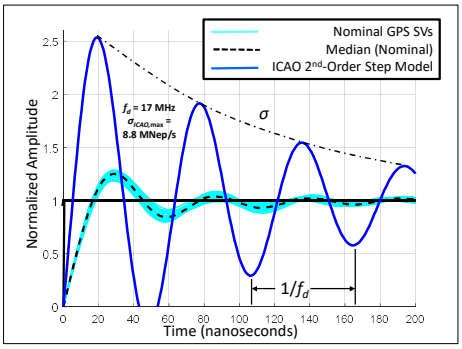

Figure 2a. *ICAO 2nd-Order Step Waveform and Parameters*

Figure 2b. *Comparison of ICAO 2OS Waveform (f_d=17 MHz , σ=8.8 MNepers/s) and nominal signals*

Still, this standard model generally provides a conservative estimate of both nominal and previously-observed anomalous signals. (Shallberg, K. et al, 2017) It has so far proven sufficient for ensuring that monitors designed to mitigate it also capable of mitigating many threats from outside that model. (Phelts, R. E. et al, 2017)

4. Extended and Amplitude modulated Model

The amplitude-scaled 2OS model was first introduced by Phelts, et al (2017), and better models nominal and near-nominal signal distortions. First, it extends the parameter ranges (e.g., σ>>8.8 MNepers/s). More significantly, it also adds an additional parameter to weight the amplitude against a theoretical "ideal", infinite bandwidth code input. This combination, however, results in a cusp in the step response. This was less imprtant for more approximate, post-correlation analyses, but for signal shape estimation it would significantly reduce model agreement with high gain dish observations.

To remedy this, a bandlimited (overdamped) code was substituted for the infinite bandwidth code. This required applying a filter to the input signal. For this analysis, the filter selected for the bandlimited input signal was a Chebyshev window FIR filter with 70 taps and 50 dB attenuation. In addition to the (4) amplitude-scaled 2OS model parameters, these filter specifics are necessary to reproduce the model waveforms.

Note that the filter selection here was not optimized beyond what was required to obtain a good fit to nominal dish data (after model parameter tuning). However, it was desired to use a non-distorting (FIR) filter with good attenuation and as few taps as required to produce it.

With the bandlimited input, tuning of the four model parameters (f_d, σ, Δ, a) produces good agreement between model and dish-measured waveforms. Figure 3a plots an overlay of model and measured waveforms for SVN 72 (PRN 08). (The difference between the two is also shown at the bottom of the plot.). The model parameters correspond to f_d=14.3 MHz, σ=29.7 MNepers/s, and Δ= 1.7 ns.

Figure 3b plots the same result for an entire single code chip to illustrate the effects of digital distortion. The digital distortion is plotted for 10 ns and 100 ns here because smaller distortions are barely visible at this scale. In fact, this leads to added computational complexity in model generation and added difficulty in estimation for nominal digital distortions.

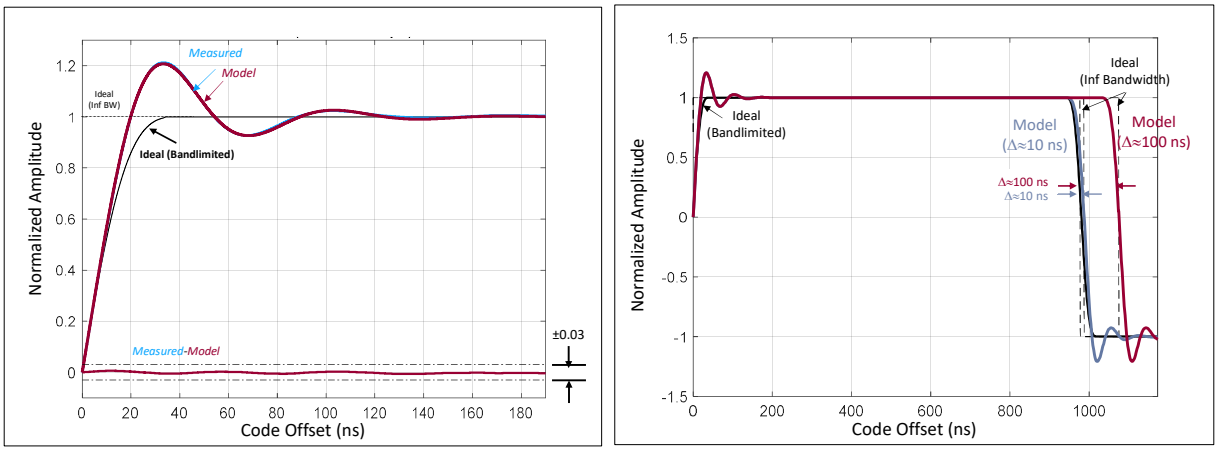

Figure 3a and 3b. *Model vs Measured signals for the amplitude-scaled 2OS model for SVN 72 (PRN 08).*

Figure 4 compares 13 model responses corresponding to the 13 dish-measured signals from 2020. (Refer to Figure 1.) The difference between measured and model was tuned be within ±0.03 for them all. Table 1 below lists the 4 amplitude-scaled 2OS model parameters corresponding to each modeled SV signal.

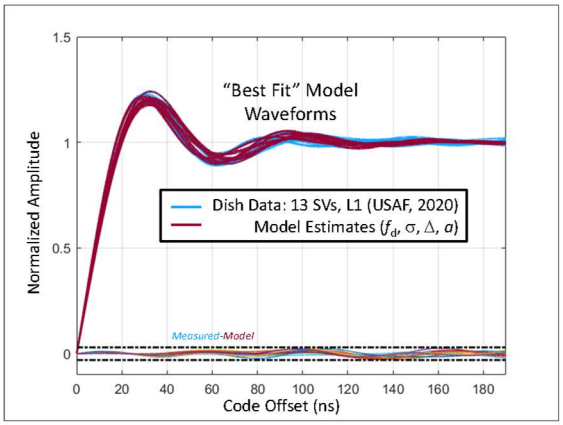

Figure 4. *Model vs Measured signals for the 13 dish-measured signals of Figure 1.*

Table 1. *Summary of parameters for the 13 dish-measured L1 /CA signals (2020) of Figure 1.*

SVN	Block Type	PRN	f_d (MHz)	σ (MNep /s)	|Δ| (ns)	a
72	IIF	8	14.3	29.7	1.7	0.33
44	IIR	28	16.0	21.05	3.40	0.48
63	IIF	1	14.4	26.2	0.63	0.41
50	IIRM	5	15.6	25.35	1.72	0.36
57	IIRM	29	15.6	24.95	1.58	0.41
43	IIR	13	16.0	19.45	2.86	0.54
58	IIRM	12	15.2	33.95	1.2	0.31
63	IIF	24	14.8	24.65	2.18	0.44
65	IIF	6	14.6	24.15	1.40	0.48
67	IIF	31	14.4	25.1	2.81	0.35
52	IIRM	10	15.5	37.4	1.43	0.19
73	III	4	14.8	27.9	2.67	0.39
74	III	18	16.7	35.4	1.86	0.02

2. WAAS Signal Quality Monitor Measurements

The WAAS signal quality monitor uses a network of 114 multi-correlator reference receivers distributed throughout North America to monitor for anomalous distortions of the correlation peak. All receivers have a bandwidth of 24 MHz. They monitor L1 correlation peaks with a total of 9 correlator outputs, including the three (Early, Late, and Prompt) used for forming the Early-minus-Late discriminator. The correlator offsets on L1 vary from -100ns to +100ns (relative to Prompt) at ~25 ns increments.

The WAAS monitor detection metrics are linear combinations of the correlator outputs and are designed to mitigate the standard 2OS threat model. (Note Phelts, R. E. et al (2017) demonstrated that the monitor is effective against more than the standard 2OS threat model.) Multiple metrics are applied to each SV being tracked. Each is referenced to the corresponding median metric across all SVs.

The full procedure for implementing the detection metrics in the WAAS signal quality monitor is described by Phelts, et al (2022). But the final (unnormalized) receiver-averaged detection metric m on L1 for SV i is referenced (adjusted) to the median metric across all SVs at each time t according to

$$ {}_{(L1)}\mathrm{D}^{i}_{m,adj}(t) = {}_{(L1)}\mathrm{D}^{i}_{m}(t) - \underset{i}{\mathrm{median}}\left({}_{(L1)}\mathrm{D}^{i}_{m}(t) \right) \tag{4} $$

2. ANALYSIS

1. Measurement-to Model Calibration

The WAAS detection metrics are referenced to the median across SVs in view of the network. (See Equation 4.). This median is the assumed undistorted, nominal signal from which signal deformation is measured. It is a relatively stable reference but in practice it can vary somewhat depending on the satellites in view. This introduces some satellite-dependent variations that require calibration to compare to models of dish measurements. Accordingly, metrics averaged over a 24-hr periods were used to calibrate the WAAS-observed metric measurements relative to the modeled dish measurements for each SV *i*.

Dish-equivalent signals are modeled using the parameters of Table 1. The procedure outlined by Phelts, et al (2015, 2022) was used to compute modeled WAAS detection metrics $[D^i_{model,"best"fit}]$ for these analytical signals. The vectors of observed (mean) WAAS metrics $[\bar{D}^i_{meas,nom}]$ were tuned to the model for each SV *i* by solving for the scale matrix, β^i in Equation (4) to account for difference between the measurements and the model. This can be a simple scaling (i.e., diagonal matrix), however a least norm solution yielded better results when applied to noisy measurement data at each epoch.

$$\left[\bar{D}^i_{meas,nom}\right]^{\mathrm{T}}[\beta^i] = \left[D^i_{model,"best"fit}\right]^{\mathrm{T}} \tag{4}$$

where,

$\bar{D}^i_{meas,nom}$ is the average vector of $\mathrm{D}^i_{m,adj}(t)$ for all metrics *m* corresponding to SV *i* over 24 hours.

$D^i_{model,"best"fit}$ is a vector of WAAS metrics computed from the waveforms approximated buy model parameters as listed in Table 1 for SV *i*.

After the scale matrices have been determined, the best fit parameters over time can be found by minimizing the error J^i over the four model parameters for each SV *i* as shown in Equation 5.

$$J^i = \min_{f_d,\sigma,\Delta,a} \left\| [D^i_{meas}(t)]^{\mathrm{T}}\beta^i - \left[D^i_{model,all}(f_d,\sigma,\Delta,a)\right]^{\mathrm{T}} \right\| \tag{5}$$

Because each SV has a slightly different scaling matrix β^i , the solution to Equation 5 can return a slighty different set of parameters. A final minimization over *i* (Equation 6) produces the parameters with the best match overall. However, the variation information also provides some measure of uncertainty or sensitivity to the different results.

$$J = \min_i(J^i) \tag{6}$$

Note that having only 13 SVs calibrated introdices some additional error. Best results would be achieved with greater numbers and diversity of signals with properly-calibrated metric measurements.

2. Computational Considerations

The minimization of Equation 5 requires a fine discretization of the amplitude-scaled 2OS model. And, to account for increased uncertainty when characterizing anomalous waveforms, it may also require wide ranging parameter limits. In this analysis the parameters were discretized according to the parameters limits in Table 2b. For comparison, the broadest parameter limits and (typical) discretization for the ICAO 2OS threat model is also shown in Table 2a.

Tables 2a and 2b. *Parameter ranges and increments for standard ICAO (left) and amplitude-scaled (right) 2OS models*

Parameter	Min	Max	Increment
f_d (MHz)	7.3	13	0.1
σ (MNep/s)	0.8	8.8	0.5
Δ (chips)	-0.12	0.12	0.01
-	-	-	-

Parameter	Min	Max	Increment
f_d (MHz)	2	25	1
σ (MNep/s)	0.8	25.3	0.5
Δ (chips)	-0.12	0.12	0.0001
a	0	1	0.1

Relative to the standard 2OS model, the addition of the amplitude factor (a) alone increases the search size by a factor of 10. Extending the limits of f_d and σ increases it further by additional factors of (approximately) 2 and 3, respectively. Most significantly, since the digital distortion parameter Δ is nominal specification usually tracked to the nanosecond or smaller, it requires a 100-fold decrease in increment size. If modeled directly, this would also require significant increase in the sample rate for generating the model waveforms. All these factors potentially greatly increase the computational cost of generating the model.

For this analysis some resolution density was sacrificed to expand the parameter limits of f_d and σ. For Δ, the 100x increase in resolution below 10 ns was achieved via interpolation. These compromises likely result in somewhat reduced model accuracy and also increase the minimum achievable error function of Equation 5 during searches but were necessary to establish initial results in a reasonable time frame.

Also note the parameter limit of the damping factor σ was just 25.3 MNepers/s. It was subsequently discovered that this was less than required for several of the 13 "best fit" model waveforms of Table 1. A significantly broader (and denser) model is anticipated in the future, but it is believed that these results are still sufficient to demonstrate the potential utility of this approach.

3. RESULTS

1. Parameter Validation

Figures 5a and 5b show the estimation of the 4 amplitude-scaled 2OS model parameters for SVN 43 (PRN 13) and SVN 72, respectively over a 24-hour day. In each case the "best fit" parameters (black) closely agree with the estimated (blue) averaged over the 24-hour period. The largest % error for most parameters was approximately 10%. The exception was for the estimate of σ on SVN 72. In that case, the σ estimate was limited by the model parameter limit, which for this scenario was too small. This did not significantly affect the estimation of the other parameters in this instance (but this does not always hold true).

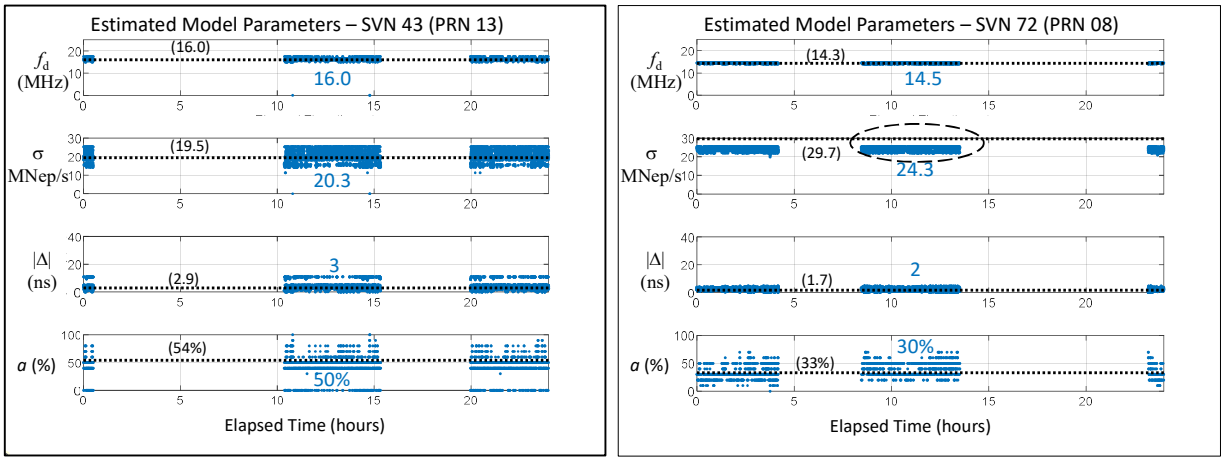

Figures 5a and 5b. *Nominal Signal Deformation Parameter Estimates for SVN 43 (PRN 13) and SVN 72 (PRN 08)*

Note that the least noisy estimate is generally the damped frequency of oscillation, f_d. The noisiest parameter estimate is usually a, followed by σ. This is likely because the both a and σ strongly affect the maximum amplitude of overshoot. Noisy measurements of course tend to make the solutions to Equation (5) converge to local erroneous parameters more frequently.

The digital distortion (Δ) parameter can prove challenging to estimate as well. The noise from other parameters complicates this. Also, at increments below ~10 ns, changes in the correlation peak shape are extremely subtle. In addition, the interpolation used to extend the model below 10 ns (with less computational cost) may "smooth" some otherwise more observable distortion. Dish measurements and receivers that track using so-called code domain observables allow far more direct estimation of this parameter. (Wong, G. et al, 2010; Pagot, J. B. et al, 2015)

Table 3a provides summary parameter estimates for 6 of the 13 SVs analyzed here. These 6 were selected because all four of the true ("best fit") parameters from Table 1 were within the parameter limits for this analysis. Table 3b shows the percent error in the estimates. As expected, despite having small cost functions, the approach has the most difficulty with very small digital distortions and sometimes with a as well. This can likely be improved by reducing the increment size for the amplitude-scale factor a, modeling small digital distortions (Δ) more precisely, and increasing the number of calibrated SVs with more (current) dish measurements.

Tables 3a and 3b. *Summary of Parameter Estimates and % Error for 6 SVs*

Parameter Estimates (6 of 13 SVs)				
PRN	**f_d (MHz)**	**σ (MNep/s)**	**|Δ| (ns)**	***a***
28	16.00	21.30	3	0.50
29	15.50	24.80	2	0.40
13	16.00	19.30	3	0.50
24	15.00	25.30	1	0.30
6	15.00	24.80	2	0.40
31	14.50	24.30	1	0.50

Parameter Estimates % Error (6 of 13 SVs)				
PRN	**f_d (% Err)**	**σ (% Err)**	**|Δ| (% Err)**	***a* (% Err)**
28	0.00	1.19	11.68	4.17
29	0.64	0.60	27.17	2.44
13	0.00	0.77	4.69	7.41
24	1.35	2.64	54.15	31.82
6	2.74	2.69	43.08	16.67
31	0.69	3.19	64.38	42.86

Note that to account for error uncertainty in practice, a range of values may be more useful than a single estimate. This is particularly true in the case of characterizing anomalous deformations, where, without high-gain dish measurements, there often is no "truth" to compare to.

2. Example Anomaly: SVN 66 (PRN 27)

On July 1, 2021 a signal deformation event occurred on SVN66 (PRN 27). Figures 6a and 6b below show the metric values relative to the threshold for each 24-hour period. This event was described in more detail by Phelts & Walter (2022). However, to date, no practical estimate of the waveform and the resulting user receiver error has been made. An initial assessment of this error is made in this section. (Note that because SVN 66 was not among the 13 that could be calibrated using dish data, both nominal and anomalous waveform parameters had to be estimated from the metric data using the methods in this paper.)

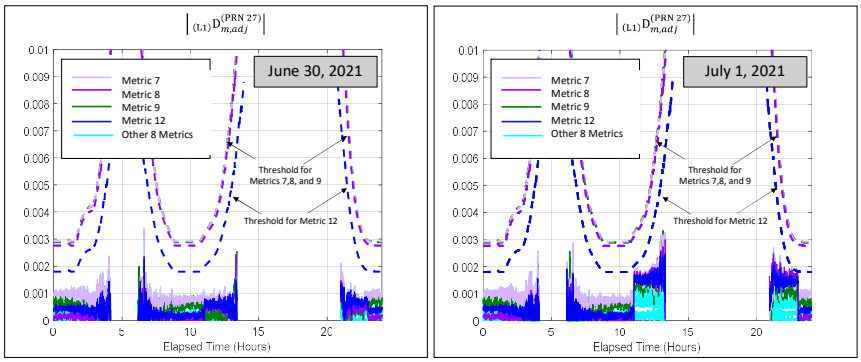

Figures 6a and 6b. *L1 WAAS metrics for SVN 66 (PRN 27) on June 30, 2021 (left) and July 1, 2021 (right)*

Parameter estimates for nominal (blue) and anomalous (maroon) are shown in Figure 7a. Based on the lowest cost function J from Equation 6, it is estimated that during the anomaly caused the signal became more oscillatory. The frequency estimate increased only slightly from 15 MHz to 16 MHz, but the damping (σ) decreased from the maximum parameter limit (or higher) significantly to just 9.3 MNepers/s. The amplitude scaling factor (a) went to zero indicating no weighting of this with an ideal (bandlimited) code. In addition, the digital distortion estimate increased from 1.5 ns to nearly just nearly 10ns—the specification for maximum nominal digital distortions on GPS signals.

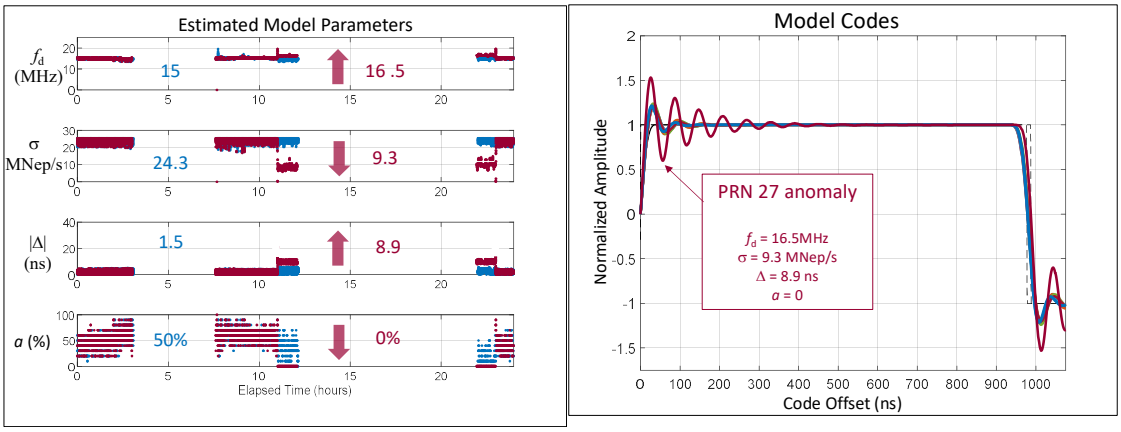

Figures 7a and 7b. *Nominal (blue) and anomalous (maroon) parameter estimates for SVN 66 (PRN 27) and waveforms*

Figure 7b plots this anomalous waveform estimate over the nominal ones of Table 1. Increased oscillations and also increased overshoot are readily observed. However, despite having no amplitude scaling, the step response is much closer to nominal than the standard ICAO waveforms of Figure 2b because the input filter is the bandlimited code.

Figure 8 plots the nominal and anomalous range error estimates from these estimated waveforms. (The range errors have been maximized over a range of WAAS user receiver configurations as described in Phelts & Walter (2022) and are detailed in the WAAS Minimum Operational Performance Standards, DO-229D).

Prior to the anomaly, the nominal differential range errors remain below 35 cm. (35 cm is the WAAS assumption for the maximum nominal user range errors.) At the time of the anomaly, the differential range errors corresponding to the lowest error function J^i rose to nearly 1 meter, and were not significantly larger even assuming the largest J^i over all 13 SVs. Without differential corrections, the likely range error was approximately 2 meters with the smallest error function. This estimate was as high as 4.7 m corresponding to parameter estimates with the largest J^i. In other words, even in the case of largest estimation uncertainty the range errors for this anomaly remained below the minimum WAAS error limits (~5 meters).

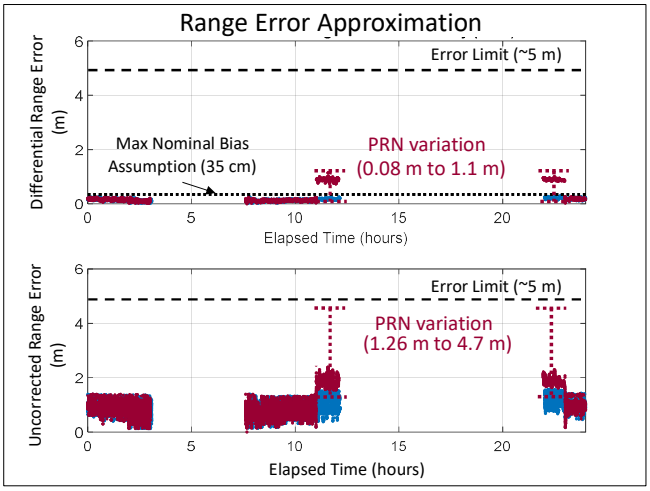

Figures 8. *Nominal (blue) and anomalous (maroon) range error estimates for SVN 66 (PRN 27)*

4. CONCLUSIONS

This paper presented a method to estimate the code waveforms from the WAAS signal monitor metric data. It leverages a more precise 4-parameter model to characterize nominal and near-nominal, anomalous signal distortions. This model does not replace the standard ICAO 2nd-order Step threat model and is not intended to do so. But it is intuitively linked to and can better approximate observed code waveform shapes.

The estimation accuracy of the techniques proposed here require proper calibration of the WAAS metrics with the model. That calibration still requires periodic high resolution, low-noise dish measurements of the signals. Estimation accuracy also depends on sufficiently broad parameter limits and fine discretization to capture the subtle signal differences.

The results show that estimation tends to be most accurate for the frequency and damping parameters. Without finer discretization, it can be somewhat less accurate for very small digital distortions << 10 ns and the for amplitude-scaling parameter, *a*. Further, while optimizing for the minimum error function produces the most likely parameter estimates, the sensitivity to errors in those estimates can be assessed by evaluating all candidate solutions across all (calibrated) SVs.

In the case of the anomaly on SVN 66 (PRN 27), the most likely range error estimates were <1 m (differential) and ~2 m (uncorrected). Assuming maximum uncertainty, the differential error estimate saw only a slight increase, but the uncorrected error estimate was as high as 4.7 m. In either case, the ranger error estimates remained below the 5-meter WAAS range error limit.

While the results presented here are promising they are not final. Additional dish-measurements for calibrated signals along with increased model density and breadth are needed for improved estimation accuracy. Also, additional validation is needed to confirm more estimation results. However, it is believed this approach can complement dish antenna measurements and provide a valuable tool for assessing the effects of signal deformations in GNSS receivers on an ongoing basis in the future.

ACKNOWLEDGMENTS

The authors would like to thank the FAA Satellite Navigation Team for funding this effort under MOA 693KA8-19-N-00015.

REFERENCES

Minimum Operational Performance Standards (MOPS) for WAAS, DO-229D. RTCA.

Pagot, J. B., Thevenon, P., Julien, O., Gregoire, Y., Amarillo-Fernandez, F., et al. (2015) Estimation of GNSS Signals' Nominal Distortions from Correlation and Chip Domain. *Proceedings of the 2015 International Technical Meeting of The Institute of Navigation, (ION ITM 2015)*, Dana Point, California, United States. ffhal-01120942

Phelts, R. E. (2001) *Multicorrelator Techniques for Robust Mitigation of Threats to GPS Signal Quality*, Ph.D. Dissertation, Stanford University, Stanford, CA

Phelts, R. E., Altshuler, E., Walter, T., Enge, P. (2015) Validating Nominal Bias Error Limits Using 4 years of WAAS Signal Quality Monitoring Data. *Proceedings of the ION 2015 Pacific PNT Meeting*, Honolulu, Hawaii, April 2015, pp. 956-963.

Phelts, R. E., Shallberg, K., Walter, T., Enge, P. (2017) "WAAS Signal Deformation Monitor Performance: Beyond the ICAO Threat Model," *Proceedings of the ION 2017 Pacific PNT Meeting*, Honolulu, Hawaii, pp. 713-724. https://doi.org/10.33012/2017.15103

Phelts, R. E., Walter, T., Enge, P. (2009) Characterizing Nominal Analog Signal Deformation on GNSS Signals. *Proceedings of the 22nd International Technical Meeting of the Satellite Division of The Institute of Navigation (ION GNSS 2009)*, Savannah, GA, pp. 1343-1350.

Phelts, R. E., Wong, G., Walter, T., Enge, P., (2013) Signal Deformation Monitoring for Dual-Frequency WAAS. *Proceedings of the 2013 International Technical Meeting of The Institute of Navigation*, San Diego, California, pp. 93-106.

Shallberg, Karl W., Ericson, S. D., Phelts, E., Walter, T., Kovach, K., Altshuler, E. (2017) Catalog and Description of GPS and WAAS L1 C/A Signal Deformation Events. *Proceedings of the 2017 International Technical Meeting of The Institute of Navigation*, Monterey, California, pp. 508-520.

Thoelert, S., Circiu, M.S., Meurer, M. (2020) Impact of Satellite Biases on the Position in Differential MFMC Applications. *Proceedings of the 2020 International Technical Meeting of The Institute of Navigation*. San Diego, California, pp. 222-235

Thoelert, S., Enneking, C., Vergara, M., Sgammini, M., Antreich, F., Meurer, M., Brocard, D., Rodriguez, C. (2015) GNSS Nominal Signal Distortions - Estimation, Validation and Impact on Receiver Performance. *Proceedings of the 28th International Technical Meeting of the Satellite Division of The Institute of Navigation (ION GNSS+ 2015)*, Tampa, Florida, pp. 1902-1923.

Wong, G. (2014) *Impact of Nominal Signal Deformations on Satellite Navigation Systems*. Ph.D. Dissertation, Stanford University, Stanford, CA

Wong, G., Phelts, R.E., Walter, T., Enge, P. (2010) Characterization of Signal Deformations for GPS and WAAS Satellites. *Proceedings of the 23rd International Technical Meeting of the Satellite Division of The Institute of Navigation (ION GNSS 2010)*, Portland, OR, pp. 3143-3151.